Probing protein–lipid interactions by FRET between membrane fluorophores

2016 Methods Appl. Fluoresc. 4 034014

(http://iopscience.iop.org/2050-6120/4/3/034014)

Methods and Applications in Fluorescence

RECEIVED
27 February 2016

REVISED
22 August 2016

ACCEPTED FOR PUBLICATION
2 September 2016

PUBLISHED
21 September 2016

PAPER

Probing protein–lipid interactions by FRET between membrane fluorophores

Valeriya M Trusova[1,3], Galyna P Gorbenko[1], Todor Deligeorgiev[2] and Nikolai Gadjev[2]

[1] Department of Nuclear and Medical Physics, V.N. Karazin Kharkiv National University, 4 Svobody Sq., Kharkiv 61022, Ukraine
[2] Faculty of Chemistry, Department of Applied Organic Chemistry, University of Sofia, 1164 Sofia, Bulgaria
[3] Address to whom any correspondence should be addressed: Valeriya M. Trusova, 19–32 Geroyev Truda Str., Kharkiv 61144, Ukraine

E-mail: valtrusova@yahoo.com

Keywords: Förster resonance energy transfer, Monte-Carlo simulation, protein–lipid interactions, lysozyme, liposomes

Abstract

Förster resonance energy transfer (FRET) is a powerful fluorescence technique that has found numerous applications in medicine and biology. One area where FRET proved to be especially informative involves the intermolecular interactions in biological membranes. The present study was focused on developing and verifying a Monte-Carlo approach to analyzing the results of FRET between the membrane-bound fluorophores. This approach was employed to quantify FRET from benzanthrone dye ABM to squaraine dye SQ-1 in the model protein–lipid system containing a polycationic globular protein lysozyme and negatively charged lipid vesicles composed of phosphatidylcholine and phosphatidylglycerol. It was found that acceptor redistribution between the lipid bilayer and protein binding sites resulted in the decrease of FRET efficiency. Quantification of this effect in terms of the proposed methodology yielded both structural and binding parameters of lysozyme-lipid complexes.

1. Introduction

Among a wide variety of fluorescence-based techniques currently used in biomedical research one of the most powerful and versatile is the Förster resonance energy transfer (FRET) [1–3]. FRET sensitivity to nanometer scale proximity relationships between the moieties acting as energy donors and acceptors renders it a unique tool for structural analysis of diverse biomolecular assemblies, particularly biological membranes [4–7]. This tool proved to be highly informative in elucidating the molecular details of the interactions between two major membrane constituents, proteins and lipids [8–10]. The problems addressed with FRET concern the mechanisms of protein–lipid binding [11, 12], conformational transitions of membrane-bound polypeptides [13, 14], lipid-assisted protein aggregation and fibrillization [15, 16], lipid lateral redistribution and domain formation [17, 18], to name only a few. The principal advantages of FRET when being applied to the membrane systems lie in: (i) experimentation within concentration range inaccessible with other techniques; (ii) sensitivity to subtle details of protein–lipid interactions; (iii) detection of molecular clusters, unamenable to other methods; (iv) providing structural information about protein and lipid membrane components under the same experimental conditions; (v) versatility and relative simplicity of the experiment. Within the past decades, the emergence of novel optical methods and instrumentation, genetically encoded fluorescent proteins, site-specific fluorescent labels and fluorophores with improved characteristics has led to a remarkable upsurge in the use of FRET technique. The progress in this field is also significantly driven by the development of new approaches to the quantification of FRET data [19–21]. The efficiency of energy transfer in membrane systems is determined by numerous factors, such as spatial arrangement of donors and acceptors in a lipid bilayer, randomness of their lateral distribution, the effect of excluded area, relative orientation of donor and acceptor, the curvature of membrane surface, etc. Theoretical background for the description of energy transfer in membranes is provided by a number of models [22–27], considering donors and acceptors randomly distributed over the infinite plane, parallel infinite planes [22–24], surfaces of concentric spheres [25], acceptor exclusion from an area around donor and interplanar separation of the donor and acceptor arrays [26, 27]. Since FRET between membrane-associated donors and acceptors can be described analytically only for the random fluorophore distribution, the prevailing current tendency consists

in the development of simulation-based data analysis approaches, implementing, particularly, Monte-Carlo algorithms. Being much more versatile and flexible, such approaches can be applied to geometric conditions of any complexity [28, 29].

In the present contribution we employed a Monte-Carlo algorithm to quantify the results of FRET measurements in the model protein–lipid system containing a basic globular protein lysozyme and negatively charged lipid vesicles composed of phosphatidylcholine and phosphatidylglycerol. A lipophilic benzanthrone dye ABM was used as an energy donor, while squaraine dye SQ-1 was recruited as an acceptor. Our goal was twofold: (i) to verify the idea that protein adsorption onto lipid bilayer may exert influence on the mutual arrangement of the donor and acceptor molecules, thereby resulting in the changes of FRET profiles; and (ii) to evaluate the possibility of obtaining quantitative information on the protein–lipid interactions through measuring FRET between membrane-incorporated fluorophores.

2. Materials and methods

2.1. Materials

Squaraine dye SQ-1 (4-[(1-butyl)-3,3-dimethyl-naphtylindole-2-yl]methylene]-2-[(butyl-3,3-dimethyl-naphtindole-2-ylidene)methyl]-3-oxo-1-cyclobuten-1-olate) was synthesized at the Faculty of Chemistry, University of Sofia [30]. ABM (3-morpholino-7H-benzo[de]anthracene-7-one) was kindly provided by Drs. Jelena Kirilova and Inta Kalnina from Daugavpils University, Latvia. The dye purity was ~98% for SQ-1 and ~95% for ABM. The chemical structure and the purity of SQ-1 were confirmed by ^{1}H NMR spectroscopy and elemental analysis. ^{1}H NMR (DMSO-d6, δ(ppm)): 0.93–1.023 q (6H, 2 × CH_3), 1.39–1.48 m (4H, 2 × CH_2), 1.69–1.79 m (4H, 2 × CH_2), 1.96 s (12H, 4 × CH_3), 4.22 t (4H, 2 × NCH_2), 5.88 s (2H, 2 × CH), 7.42–8.24 m (12H, Ar). Elemental analysis for C42H44N2O2·1.5 H2O: calc.: C 79.34%, H 7.45%, N 4.41%; found: C 80.08%, 7.10%, N 4.90%. Mp 272–274 °C. The chromatomass spectroscopic studies of ABM were carried out using Shimadzu GCMS-QP2010 system (Shimadzu Corporation, Kyoto, Japan).The gas chromatograph was equipped with an electronically controlled split/splitless injection port. Gas chromatography was carried out on a 5% diphenyl-/95% dimethylpolysiloxane fused-silica capillary column (Rtx-5SIL-MS, 30 m × 0.32 mm, 0.25 μm film thickness; Restek). Helium (99.999%) was used as the carrier gas at a constant flow of 1.6 ml min^{-1}. The injection (injection volume of 1 μl) was performed at 250 °C in the split mode, with the split ratio 1:10. The mass spectrometer was operated in the electron ionization mode (ionization energy 70 eV). The detection was carried out in the scan mode: m/z 39–400. The dye purification was achieved using high performance accelerated chromatographic isolation system Isolera One with detectors: UV1 (collection) 400 nm, UV2 (monitor) 254 nm; cartridge type SNAP 10 g; solvents system—*n*-hexane:ethyl acetate 1:1.

Egg yolk phosphatidylcholine (PC) and phosphatidylglycerol (PG) were purchased from Avanti Polar Lipids (Alabaster, AL). Chicken egg white lysozyme was from Sigma (St. Louis, MO, USA). All other chemicals were of analytical grade and used without further purification.

2.2. Preparation of lipid vesicles

Unilamellar lipid vesicles composed of neat PC and its mixtures with 20 mol% PG were prepared by the extrusion method [31]. Appropriate amounts of lipid stock solutions were mixed in ethanol, evaporated to dryness under a gentle nitrogen stream, and then left under reduced pressure for 1.5 h to remove any residual solvent. The obtained thin lipid films were hydrated with 1.2 ml of 5 mM sodium-phosphate buffer (pH 7.4) at room temperature. Thereafter lipid suspensions were extruded through a 100 nm pore size polycarbonate filter (Nucleopore, Pleasanton, CA. The phospholipid concentration was determined according to the procedure of Bartlett [32].

2.3. Fluorescence measurements

Steady-state fluorescence spectra were recorded with LS-55 spectrofluorimeter equipped with a magnetically stirred, thermostated cuvette holder (Perkin-Elmer Ltd., Beaconsfield, UK). Fluorescence measurements were performed at 20 °C using 10 mm path-length quartz cuvettes. Excitation and emission slit widths were 10 nm. Excitation wavelengths for ABM was 430 nm.

The stock solutions of SQ-1 (56 μM) and ABM (480 μM) were prepared in ethanol. The dye concentrations were determined spectrophotometrically, using the extinction coefficients $\varepsilon_{663} = 2.3 \times 10^5$ M^{-1} cm^{-1} (SQ-1) and $\varepsilon_{444} = 2.1 \times 10^4$ M^{-1} cm^{-1} (ABM). 5 μl of ABM stock solution was added to 200 μl of the concentrated liposome suspension (2 mM) and incubated for half an hour at room temperature to allow the dye to partition into the liposomal membranes. Then, the above ABM-liposome mixture was diluted with 1.3 ml of 5 mM sodium-phosphate buffer (pH 7.4) and 200 μl portions of this solution were mixed with appropriate amounts (from 0 to 200 μl) of SQ-1 stock solution in ethanol 6-fold diluted with buffer. After a 30 min incubation at room temperature the volume of each sample was increased to 2.1 ml by adding the required amounts of buffer solution. Finally, 2 ml of each of the above samples was placed into fluorimetric cuvette and fluorescence spectra were recorded in the absence of lysozyme and at increasing the protein concentration. In this way, we acquired 2D datasets of the relative fluorescence intensity of ABM measured for six SQ-1 concentrations (from 0.09 to 0.89 μM) and five protein concentrations (from 0.07 to 0.34 μM).

Fluorescence intensity of ABM measured in the presence of SQ-1 was corrected for the inner filter effects using the following coefficients [33]:

$$k = \frac{(1-10^{-A^{ex}_{ABM}})(A^{ex}_{ABM}+A^{ex}_{SQ\text{-}1})(1-10^{-A^{em}_{ABM}})(A^{em}_{ABM}+A^{em}_{SQ\text{-}1})}{(1-10^{-(A^{ex}_{ABM}+A^{ex}_{SQ\text{-}1})})A^{ex}_{ABM}(1-10^{-(A^{em}_{ABM}+A^{em}_{SQ\text{-}1})})A^{em}_{ABM}} \quad (1)$$

where A^{ex}_{ABM} and A^{em}_{ABM} are the ABM optical densities at the excitation (430 nm) and emission (580 nm) wavelengths in the absence of SQ-1, and $A^{ex}_{SQ\text{-}1}$ and $A^{em}_{SQ\text{-}1}$ are the SQ-1 optical densities at the excitation and emission wavelengths, respectively.

The experimental value of the relative fluorescence intensity (I^e_r) and FRET efficiency (E) were determined as:

$$I^e_r = \frac{I_{DA}}{I_D}; \quad E = 1 - \frac{I_{DA}}{I_D} \quad (2)$$

where I_D, I_{DA} are the donor fluorescence intensities in the absence and presence of acceptor.

The critical distance of energy transfer (Förster radius) was calculated as [34]:

$$R_o = 979(\kappa^2 n_r^{-4} Q_D J)^{1/6},$$
$$J = \int_0^\infty F_D(\lambda)\varepsilon_A(\lambda)\lambda^4 d\lambda \Big/ \int_0^\infty F_D(\lambda)d\lambda \quad (3)$$

where J is the overlap integral derived from numerical integration, $F_D(\lambda)$ is the donor fluorescence intensity, $\varepsilon_A(\lambda)$ is the acceptor molar absorbance at the wavelength λ, n_r is the refractive index of the medium ($n_r = 1.4$), Q_D is the donor quantum yield that was estimated to be 0.15, κ^2 is an orientation factor. Assuming random reorientation of the donor emission and acceptor absorption transition moments during the emission lifetime ($\kappa^2 = 0.67$) the Förster radius for the examined donor–acceptor pair ABM—SQ-1 was evaluated to be 3.5 nm.

3. Results and discussion

3.1. The binding of ABM and SQ-1 to lipid membranes

The first stage of the study was aimed at the characterization of the lipid-associating properties of the employed donor and acceptor fluorophores. To this end, the dye fluorescence spectra were recorded in liposome suspension at increasing lipid concentration. As shown in figure 1, the partitioning of ABM and SQ-1 into lipid bilayer is followed by a substantial enhancement of the dye fluorescence. Such an effect is usually interpreted in terms of the decreased rate of non-radiative relaxation processes in a membrane environment where fluorophore rotation is considerably hindered resulting in a dramatic increase of its quantum yield [35]. According to our estimates, the quantum yields of ABM and SQ-1 in the PC/PG (4:1) bilayer attain the values 0.15 and 0.6, respectively. To quantitatively characterize the membrane association of the examined fluorophores we employed the partition model allowing to describe the dye distribution between aqueous and lipid phases using a parameter, such as partition coefficient (K_P) [36]:

$$K_P = \frac{Z_L V_W}{Z_W V_L}; \quad Z_{tot} = Z_W + Z_L \quad (4)$$

where Z_{tot} is the total concentration of the dye; Z_W, Z_L denote the concentrations of free and lipid-bound dye; V_W, V_L are the volumes of aqueous and lipid phases, respectively. It is easy to show that:

$$Z_L = \frac{Z_{tot} V_L K_P}{V_W + K_P V_L} \quad (5)$$

The dye fluorescence intensity measured at a certain lipid concentration (I_L) is given by:

$$I_L = a_L Z_L + a_W(Z_{tot} - Z_L)$$
$$= \frac{I_{max} Z_L}{Z_{tot}} + \frac{I_W}{Z_{tot}}(Z_{tot} - Z_L) \quad (6)$$
$$I_W = a_W Z_{tot}; \quad I_{max} = a_L Z_{tot}$$

where I_W is the dye fluorescence intensity in a buffer; I_{max} is the limit fluorescence in a membrane environment; a_W, a_L represent molar fluorescence, i.e. fluorescence intensity of one mole of the dye, free in solution and in a lipid bilayer, respectively. The fluorescence intensity increase (ΔI) upon the dye transfer from water to lipid phase can be written as:

$$\Delta I = I_L - I_W = \frac{I_{max} Z_L}{Z_{tot}} + \frac{I_W}{Z_{tot}}(Z_{tot} - Z_L) - I_W$$
$$= \frac{V_L K_P (I_{max} - I_W)}{V_W + V_L K_P} \quad (7)$$

The volume of lipid phase can be determined from:

$$V_L = N_A C_L \sum v_i f_i \quad (8)$$

where C_L is the molar lipid concentration, f_i is the mole fraction of the ith bilayer constituent, v_i is the molecular volume taken as 1.58 nm^3 for PC and PG [37]. Given that under the employed experimental conditions the volume of lipid phase is much less than the total volume of the system V_t, we assumed that $V_W \approx V_t = 1$ dm^3. The approximation of the experimental dependencies $\Delta I(C_L)$ (figures 1(B) and (D)) by the equations (7) and (8) allowed us to estimate the partition coefficients for ABM and SQ-1 and the limit fluorescence I_{max} (table 1). These estimates were further used to calculate the amount of the membrane-bound dye according to equation (5).

3.2. Measuring FRET between ABM and SQ-1 in lipid and lysozyme-lipid systems

The second stage of the study was focused on the measurement of FRET between membrane-associated ABM and SQ-1 in the absence and presence of lysozyme. Due to the overlap between ABM emission and SQ-1 absorption spectra (figure 2, inset), ABM incorporated in the lipid bilayer can act as an effective energy donor for SQ-1 with the Förster radius calculated

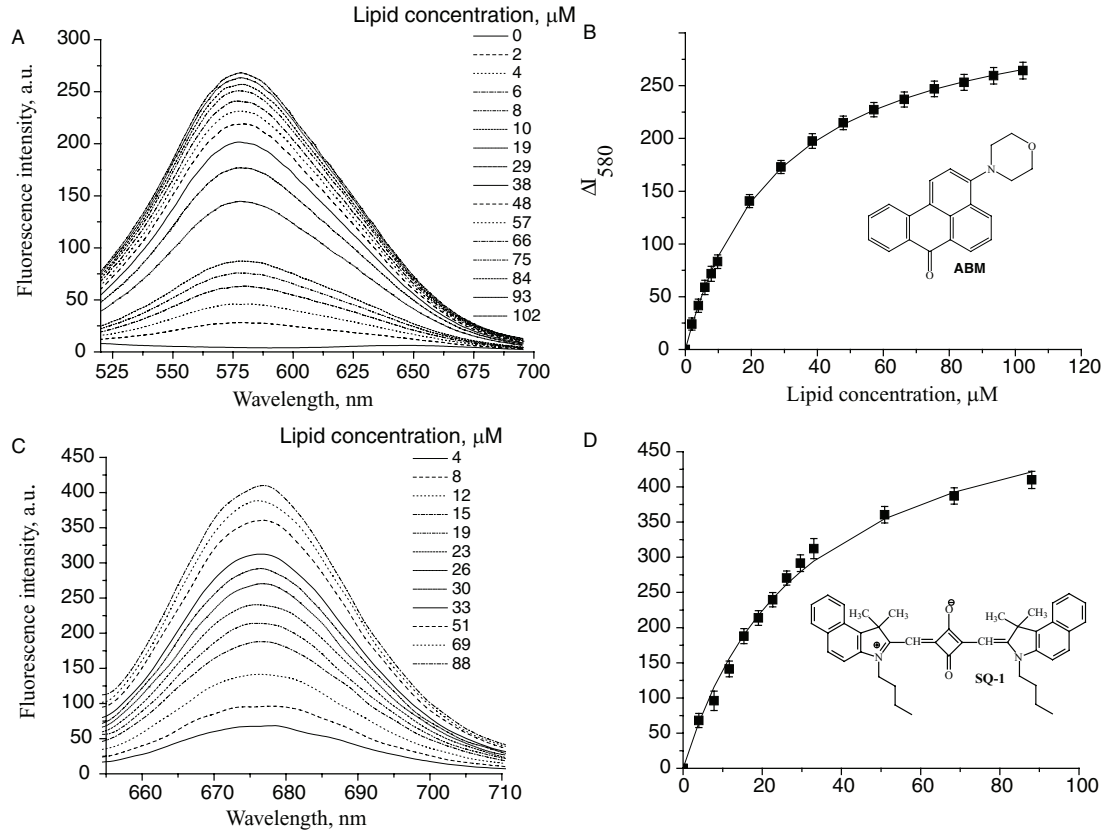

Figure 1. (A) ABM fluorescence spectra in phosphatidylcholine/phosphatidylglycerol (4:1, mol:mol) liposomes. ABM concentration was 0.5 μM. (B) The isotherm of ABM binding to PC/PG liposomes, $\Delta I = I_L - I_W$, I_W is the dye fluorescence intensity in a buffer; I_L is the fluorescence intensity measured at a certain lipid concentration. (C) SQ-1 fluorescence spectra in PC/PG liposomes. SQ-1 concentration was 0.08 μM. Emission spectrum of SQ-1 in buffer is not presented because of near-zero values of fluorescence intensity. (D) The isotherm of SQ-1 binding to PC/PG liposomes.

Table 1. Parameters of ABM and SQ-1 binding to PC:PG (4:1) liposomes.

System	Partition coefficient, K_P	Limit fluorescence, I_{max}
ABM	$(3.75 \pm 0.5) \times 10^4$	338 ± 54
SQ-1	$(3.42 \pm 0.6) \times 10^4$	568 ± 86

to be ~3.5 nm. As illustrated in figure 3, energy transfer manifests itself in a significant reduction of ABM fluorescence (with emission maximum at ~580 nm) and enhancement of SQ-1 fluorescence (with maximum at ~677 nm) at the donor excitation wavelength (430 nm). It seemed of interest to ascertain whether FRET in this donor–acceptor pair is sensitive to the membrane-related processes, particularly, to protein–lipid interactions. It might be expected that protein binding to the lipid bilayer with incorporated fluorophores would affect the pattern of membrane distribution of donors and acceptors, thus causing the changes in FRET efficiency. To test the validity of this idea, we measured FRET between ABM and SQ-1 in the model lysozyme-lipid systems. A series of samples, containing PC/PG liposomes doped with identical amounts of ABM and varying concentrations of SQ-1 were titrated with lysozyme. It appeared that increasing the extent of membrane coverage by lysozyme resulted in FRET attenuation, with the magnitude of this effect becoming more pronounced with increasing the amount of acceptor molecules. As seen in figure 4, at the maximum employed concentration of SQ-1 the increase of ABM relative fluorescence intensity compared to the protein-free liposomal systems exceeds 40%. This finding supports the above hypothesis that proteins are capable of altering the distribution of membrane-bound donors and acceptors.

3.3. Quantification of FRET in lipid system using Monte-Carlo algorithm

To interpret the observed effects quantitatively, at the third stage of the study we developed a Monte Carlo algorithm for calculating the relative fluorescence intensity of the donor in the absence of protein. The membrane-associated donors and acceptors were regarded as being confined to the planes parallel to the membrane surface and located at certain distances d_D and d_A from the bilayer center, as schematically illustrated in figure 5(A). The positions of the donors and acceptors were generated randomly in a square cell assuming periodic boundary conditions to avoid edge effects. The theoretical value of the relative fluorescence intensity (I_r^t) of the donor was calculated from the fluorophore coordinates as:

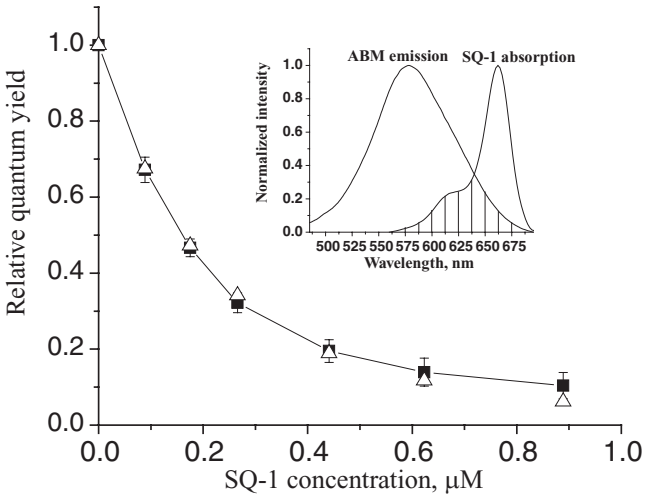

Figure 2. Relative fluorescence intensity of ABM measured as a function of SQ-1 concentration in PC/PG bilayer (solid squares) or calculated using the Monte-Carlo algorithm (hollow triangles) for the case when the donors and acceptors reside in the same plane. Shown in inset is the overlap between the ABM emission and SQ-1 absorption spectra.

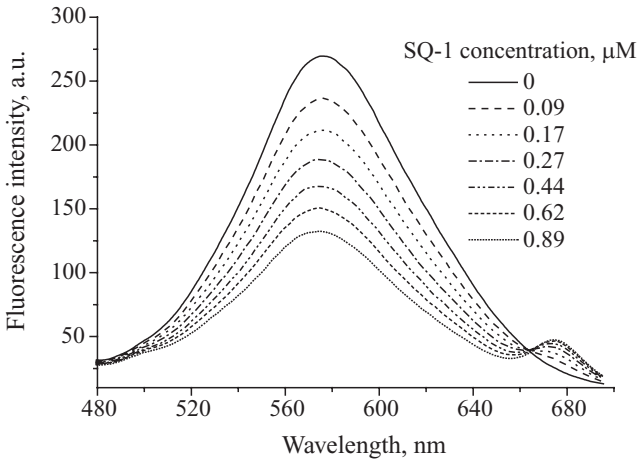

Figure 3. ABM fluorescence spectra in the system PC/PG + lysozyme recorded at varying concentrations of SQ-1. Lipid concentration was 25 μM, ABM concentration was 0.15 μM, protein concentration was 0.07 μM.

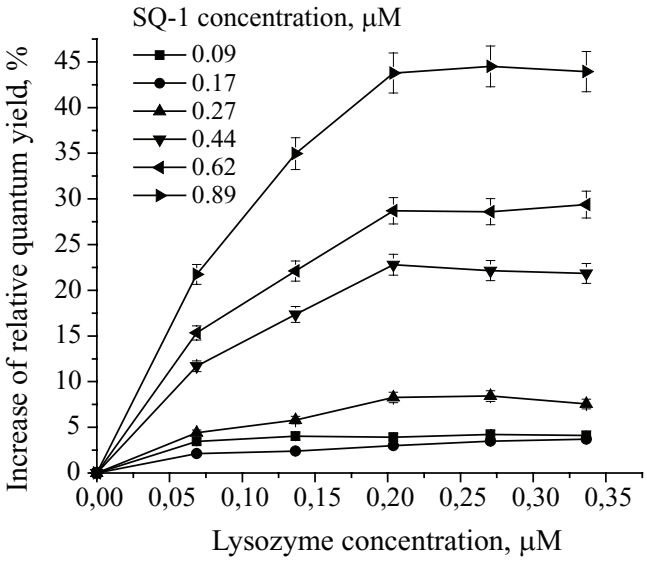

Figure 4. Increase of ABM relative fluorescence intensity as a function of lysozyme concentration. Lipid concentration was 25 μM.

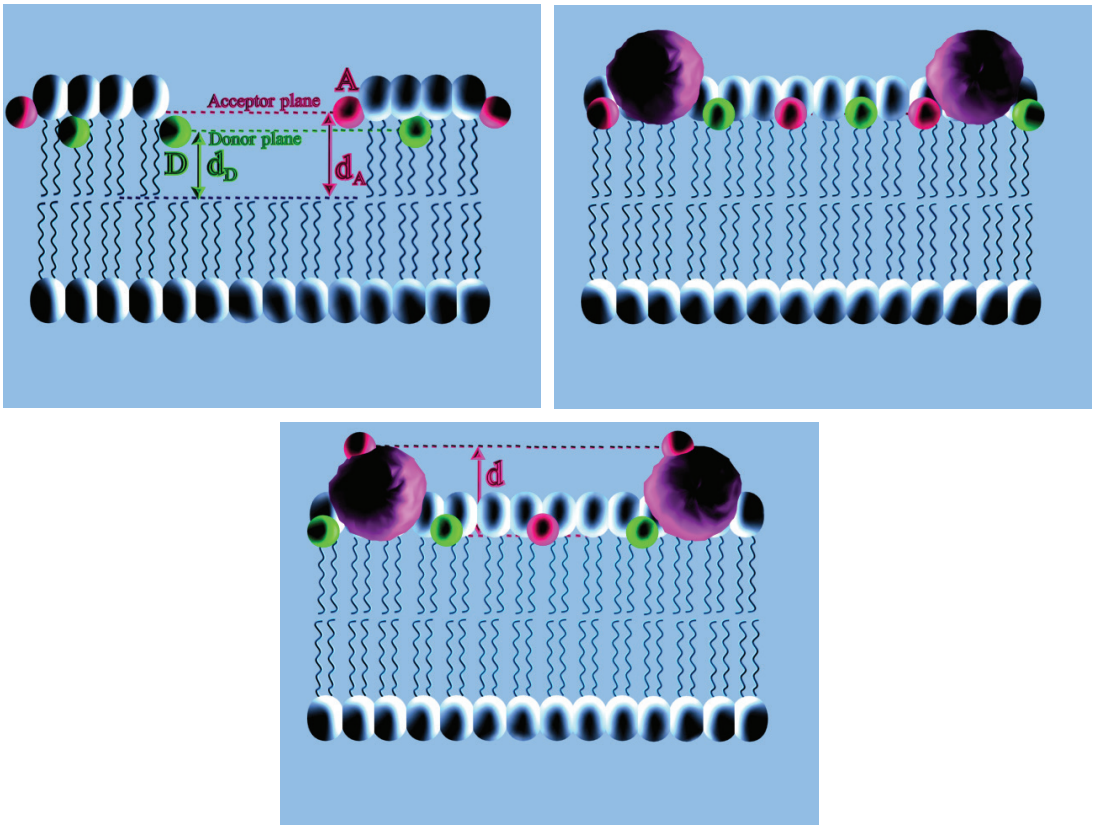

Figure 5. Schematic representation of the arrangement of donors and acceptors in a lipid bilayer. (A) The donors and acceptors are distributed at the planes parallel to the membrane surface and separated from the bilayer center by the distances d_D and d_A, respectively. (B) The donors and acceptors are forced out from the areas of the protein–lipid contacts. (C) The acceptors are distributed between the protein and lipid phases, with the protein-bound fluorophores being separated from the bilayer donor-acceptor plane by a certain distance d.

$$I_r^t = \frac{1}{N_{DL}} \sum_{j=1}^{N_{DL}} \left[1 + \sum_{i=1}^{N_{AL}} \left(\frac{R_o}{r_{ij}} \right)^6 \right]^{-1} \qquad (9)$$

where r_{ij} is the distance between jth donor and ith acceptor; N_{DL}, N_{AL} stand for the number of donors and acceptors in the cell given by:

$$N_{DL} = B_{DL} S_c / L_a S_L; \qquad N_{AL} = B_{AL} S_c / L_a S_L \qquad (10)$$

here S_c is the cell square; L_a is the concentration of accessible lipids related to the total lipid concentration (L) as $L_a = 0.5L$; S_L is the mean area per lipid molecule (taken as 0.65 nm^2 for PC and PG), R_o is the Förster radius; B_{DL}, B_{AL} are the molar concentrations of the membrane-bound ABM and SQ-1 calculated from the equation(5) using the partition coefficients presented in table 1. First, we have performed simulation of FRET in the absence of protein. The data fitting procedure was based on the minimization of the following error function:

$$f = \frac{1}{N} \sum_{i=1}^{N} (I_{ri}^e - I_{ri}^t)^2 \qquad (11)$$

where N is the number of experimental points. It was found that the best agreement between experimental and calculated values of the relative fluorescence intensity is obtained on the assumption that the donors and acceptors are distributed in the same plane, i.e. $d_D = d_A$. This is quite possible, since zwitterionic in nature chromophore of SQ-1 is supposed to reside in the polar bilayer region, while butyl tails penetrate the hydrophobic core, being oriented parallel to the lipid acyl chains [30]. ABM, similar to its well-characterized analogue 3-methoxybenzanthrone, is most likely located in the vicinity of carbonyl groups of phospholipids [38]. Thus, in the absence of protein the membrane-associated donors and acceptors can be regarded as being confined to the polar/nonpolar boundary of a lipid bilayer.

3.4. Quantification of FRET in lipid–protein system using Monte-Carlo algorithm

At the last stage of the study the above Monte-Carlo approach was extended to allow for the protein effect on the efficiency of energy transfer between the examined fluorophores. Along with calculating the amounts of the donors and acceptors, the proposed approach requires knowing the number of the protein molecules in the simulation box. This implies that the FRET formalism must be combined with the formalism of a certain adsorption model yielding an estimate of the surface density of the membrane-associated protein. The most common Langmuir adsorption model is not strictly suitable for this purpose since it does not allow for the peculiarities of protein–lipid interactions,

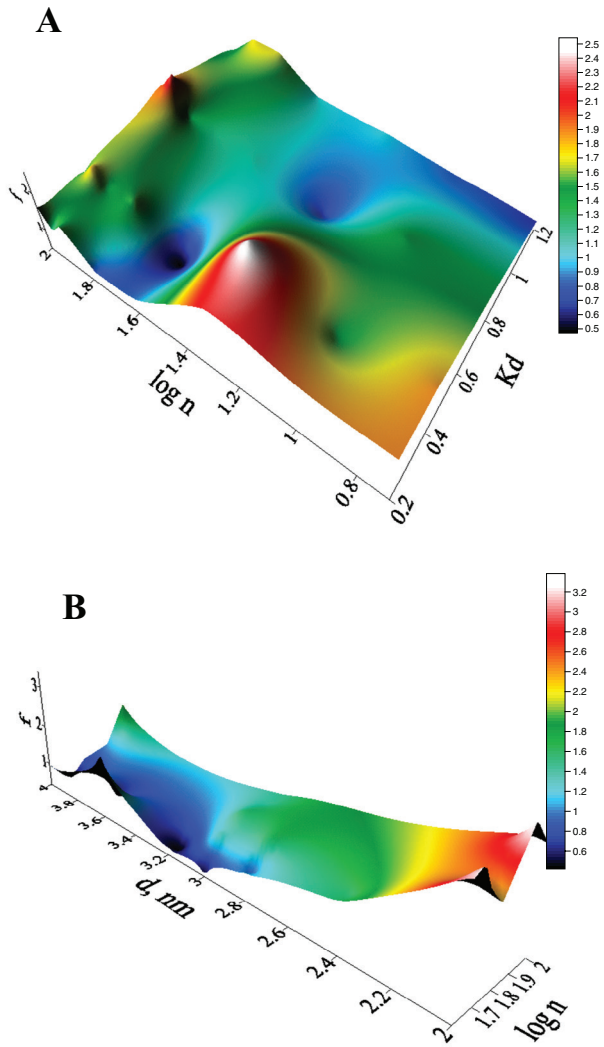

Figure 6. 3D diagram, illustrating: (A) the dependence of error function f on the parameters of lysozyme binding to PC/PG liposomes, dissociation constant K_d is given in μM, the f values (z-axis) are given as $f \times 10^3$, $d = 3$ nm; (B) the dependence of error function on log n and d at $K_d = 0.4$ μM.

such as steric area-excluding interactions between the adsorbed protein molecules and strong dependence of the binding process on a ligand shape, i.e. on the geometrical arrangement of the protein–lipid contacts [39]. These peculiarities are taken into account, particularly, in the lattice adsorption models providing a more correct description of the protein-membrane binding [40]. For globular proteins, like lysozyme, the most appropriate lattice model is described by the following equation:

$$F_P K_a = \frac{r}{1-nr}\exp\left(\frac{\alpha n r}{1-\omega r}\right); \qquad r = \frac{B_P}{L} \tag{12}$$

where B_P, F_P are the concentrations of bound and free protein, respectively; K_a is the dissociation constant; n is the number of lipid molecules per molecule of the bound protein; L is the total lipid concentration; α is the parameter of excluded area ($\alpha = 3$), $\omega = 2\sqrt{3}\,n/\pi$. The value of B_P obtained by numerical solving of the equation (12) for a certain set of parameters $\{K_a, n\}$ was further used for calculating the amount of protein molecules in the simulation cell (N_{PL}):

$$N_{PL} = B_P S_c / L_a S_L \tag{13}$$

To interpret the observed reduction of FRET resulted from the lysozyme-membrane binding, we initially assumed that protein adsorption onto lipid bilayer renders some regions, corresponding to the cross-section of the protein molecules within the plane of fluorophore distribution, inaccessible to the donor and acceptors (figure 5(B)). However, in this case we failed to reproduce the experimental FRET profiles. Therefore, it was supposed that: (i) the acceptors are distributed between the protein and lipid binding sites, and (ii) protein-bound fluorophores are separated from the bilayer donor-acceptor plane by a certain distance d (figure 5(C)). Our goal was to ascertain whether there exist the parameter sets $\{K_a, n, d\}$ at which the function f reaches its minimum. Using a Monte-Carlo algorithm the relative fluorescence intensity of the donor was calculated from equation (9) for experimentally employed combinations of the acceptor and protein concentrations (30 experimental points) with preset values of the optimizing parameters K_a, n and d. As shown in figure 6, a clear minimum of the error function, i.e. the

best agreement between theory and experiment, was observed at quite reasonable values of the optimizing parameters: $K_a \sim 2.5^{\pm 0.3}\ \mu M^{-1}$, $n \sim 40^{\pm 5}$ and $d \sim 3.2^{\pm 0.2}$ nm. Since SQ-1 resides presumably at the distance *ca.* 1 nm from the membrane surface, the recovered d estimate is consistent with the assumption that lysozyme, whose diameter is ~3 nm, penetrates into PC/PG bilayer till the level of glycerol backbone and initial carbons of acyl chains. This finding is in concert with the idea that lysozyme, despite its polycationic nature, is capable of penetrating into nonpolar membrane region [40, 41].

The present study indicates that even the simplest format of steady-state FRET measurements involving membrane-associated donor and acceptor fluorophores can provide valuable information about the structure of protein–lipid assemblies. The main steps of the proposed Monte-Carlo approach to analyzing the results of FRET measurement in the model protein–lipid systems can be summarized as follows: (i) fluorimetric titration of the dyes recruited as a donor and as an acceptor with the model lipid membranes; (ii) quantification of the dye partitioning into lipid phase; (iii) evaluation of the amount of donors and acceptors in the simulation cell; (iv) generation of the donor and acceptor coordinates in the lipid bilayer; (v) calculation of the relative fluorescence intensity of the donor for varying separation of the donor and acceptor planes; (vi) determination of the distance between donor and acceptor planes providing the best fit of the experimental FRET data in the lipid system; (vii) combination of FRET formalism with the formalism of the adsorption model describing the protein-membrane binding; (viii) calculation of the relative fluorescence intensity of the donor for a given pattern of acceptor distribution in the protein–lipid system; (ix) evaluation of the structural and binding parameters ensuring the best agreement between experiment and theory. Remarkably, the dependence of FRET efficiency on the surface concentration and distribution pattern of the acceptor molecules makes FRET technique suitable for determination of not only structural parameter (protein position relative to lipid-water interface) but also the binding parameters (dissociation constant and the number of lipids per bound protein).

It should also be noted that while analyzing the results presented here the donors and acceptors were supposed to be randomly distributed in the membrane, despite the possibility of the dye aggregation in a lipid phase cannot be excluded. In principle, the flexibility of Monte-Carlo approach allows to take into account such a possibility, but this point requires special consideration and will be a focus of our future investigation.

4. Conclusions

The measurement of resonance energy transfer between fluorescent dyes ABM and SQ-1 showed that lysozyme binding to PC/PG model membranes is accompanied by the increase of the relative fluorescence intensity compared to the neat PC/PG bilayer. This effect was quantitatively interpreted in terms of the Monte-Carlo approach based on the minimization of the difference between the experimental and calculated relative fluorescence intensities of the donor. The best fit of the experimental FRET data was achieved with the following values of the optimizing parameters: protein–lipid association constant, *ca.* 2.5 μM^{-1}, binding stoichiometry, *ca.* 40 lipid molecules per molecule of bound protein and the separation of the protein-bound acceptors from the bilayer-incorporated donors, *ca.* 3.2 nm. It was demonstrated that analysis of FRET between membrane fluorophores may prove useful in monitoring the process of protein–lipid binding accompanied by the acceptor redistribution between the lipid and protein phases.

References

[1] Selvin P R 2000 The renaissance of fluorescence resonance energy transfer *Nat. Struct. Biol.* **7** 730–4

[2] Giepmans B N G, Adams S R, Ellisman M H and Tsien R Y 2006 The fluorescent toolbox for assessing protein location and function *Science* **312** 217–24

[3] Raicu V and Singh D R 2013 FRET spectrometry: a new tool for the determination of protein quaternary structure in living cells *Biophys. J.* **105** 1937–45

[4] Loura L and Fedorov A 2000 Partition of membrane probes in a gel/fluid two-component lipid system: a fluorescence resonance energy transfer study *Biochim. Biophys. Acta* **1467** 101–12

[5] Wong A P and Groves J T 2002 Molecular topography imaging by intermembrane fluorescence resonance energy transfer *Proc. Natl Acad. Sci. USA* **99** 14147–52

[6] Silvius J R and Nabi I R 2006 Fluorescence-quenching and resonance energy transfer studies of lipid microdomains in model and biological membranes *Mol. Membr. Biol.* **23** 5–16

[7] Loura L and Prieto M 2011 FRET in membrane biophysics: an overview *Front. Physiol.* **92** 1–11

[8] Nazarov P V, Koehorst R B, Vos W L, Apanasovich V V and Hemminga M A 2006 FRET study of membrane proteins: simulation-based fitting for analysis of membrane protein embedment and association *Biophys. J.* **91** 454–66

[9] Hoppe A, Christensen K and Swanson J A 2002 Fluorescence resonance energy transfer-based stoichiometry in living cells *Biophys. J.* **83** 3652–64

[10] Nazarov P V, Koehorst R B M, Vos W L, Apanasovich V V and Hemminga M A 2007 FRET study of membrane proteins: determination of the tilt and orientation of the N-terminal domain of M13 major coat protein *Biophys. J.* **92** 1296–305

[11] Subramanian M, Jutila A and Kinnunen P K J 1998 Binding and dissociation of cytochrome c to and from membranes containing acidic phospholipids *Biochemistry* **37** 1394–402

[12] Corbalan-Garcia S, Sanchez-Carrillo S, Garcia-Garcia J and Gomez-Fernandez J C 2003 Characterization of the membrane binding mode of the C_2 domain of PKCε *Biochemistry* **42** 11661–8

[13] Calleja V, Ameer-Beg S M, Vojnovic B, Woscholski R, Downward J, Larijani B 2003 Monitoring conformational changes of proteins in cells by fluorescence lifetime imaging microscopy *Biochem. J.* **372** 33–40

[14] Chigaev A, Buranda T, Dwyer D C, Prossnitz E R and Sklar L A 2003 FRET detection of cellular α_4-integrin conformational activation *Biophys. J.* **85** 3951–62

[15] Yano Y, Takemoto T, Kobayashi S, Yasui H, Sakurai H, Ohashi W, Niwa M, Futaki S, Sugiura Y and Matsuzaki K 2002 Topological stability and self-association of a completely hydrophobic model transmembrane helix in lipid bilayers *Biochemistry* **41** 3073–80

[16] You M, Li E, Wimley W C and Hristova K 2005 Förster resonance energy transfer in liposomes: measurements of transmembrane helix dimerization in the native bilayer environment *Anal. Biochem.* **340** 154–64
[17] Brown A C, Towles K B and Wrenn S P 2007 Measuring raft size as a function of membrane composition in PC-based systems: part I- binary systems *Langmuir* **23** 11180–7
[18] Loura L M S, Fernandes F and Prieto M 2010 Membrane microheterogeneity: Förster resonance energy transfer characterization of lateral membrane domains *Eur. Biophys. J.* **39** 589–607
[19] Fernandes F, Loura L M, Koehorst R, Spruijt R B, Hemminga M A, Fedorov A and Prieto M 2004 Quantification of protein–lipid selectivity using FRET: application to the M13 major coat protein *Biophys. J.* **87** 344–52
[20] VanBeek D B, Zwier M C, Shorb J M and Krueger B P 2007 Fretting about FRET: correlation between *k* and *R Biophys. J.* **92** 4168–78
[21] Shoura M J, Udayana Ranatunga R J K, Harris S A, Nielsen S O and Levene S D 2014 Contribution of fluorophore dynamics and solvation to resonant energy transfer in protein-DNA complexes: a molecular-dynamics study *Biophys. J.* **107** 700–10
[22] Fung B and Stryer L 1978 Surface density determination in membranes by fluorescence energy transfer *Biochemistry* **17** 5241–8
[23] Estep T and Thompson T 1979 Energy transfer in lipid bilayers *Biophys. J.* **26** 195–208
[24] Wolber P and Hudson B 1979 An analytic solution to the Förster energy transfer problem in two dimensions *Biophys. J.* **28** 197–210
[25] Dewey T and Hammes G 1980 Calculation of fluorescence resonance energy transfer on surfaces *Biophys. J.* **32** 1023–36
[26] Doody M, Sklar L, Pownall H, Sparrow J, Gotto A and Smith L A 1983 A simplified approach to resonance energy transfer in membranes, lipoproteins and spatially restricted systems *Biophys. Chem.* **17** 139–52
[27] Gutierrez-Merino G, Munkonge F, Mata A, East J, Levinson B, Napier R and Lee A 1987 The position of ATP binding site on the $(Ca^{2+} + Mg^{2+})$-ATPase *Biochim. Biophys. Acta* **897** 207–16
[28] Berney C and Danuser G 2003 FRET or no FRET: a quantitative comparison *Biophys. J.* **84** 3992–4010
[29] Corry B, Jayatilaka D and Rigby P 2005 A flexible approach to the calculation of resonance energy transfer efficiency between multiple donors and acceptors in complex geometries *Biophys. J.* **89** 3822–36
[30] Ioffe V, Gorbenko G, Deligeorgiev T, Gadjev N and Vasilev A 2007 Fluorescence study of protein–lipid complexes with a new symmetric squarylium probe *Biophys. Chem.* **128** 75–86
[31] Mui B, Chow L and Hope M J 2003 Extrusion technique to generate liposomes of defined size *Methods Enzymol.* **367** 3–14
[32] Bartlett G 1959 Phosphorus assay in column chromatography *J. Biol. Chem.* **234** 466–8
[33] Bulychev A A, Verchoturov V N and Gulaev B A 1988 *Current Methods of Biophysical Studies* (Moscow: Vyschaya shkola)
[34] Lakowicz J R 2006 *Principles of Fluorescent Spectroscopy* 3rd edn (New York: Springer)
[35] Zhang D, Zhao Y, Qiao Z, Mayerhoffer U, Spenst P, Li X, Wurthner F and Wang H 2014 Nano-confined squaraine dye assemblies: new photoacoustic and near-infrared fluorescence dual-modular imaging probes *in vivo Bioconjug. Chem.* **25** 2021–9
[36] Santos N, Prieto M and Castanho M 2003 Quantifying molecular partition into model systems of biomembranes: an emphasis on optical spectroscopic methods *Biochim. Biophys. Acta* **1612** 123–35
[37] Ivkov V G and Berestovsky G N 1981 *Dynamic Structure of Lipid Bilayer* (Moscow: Nauka)
[38] Dobretsov G E 1989 *Fluorescent Probes in the Studies of Cells, Membranes and Lipoproteins* (Moscow: Nauka)
[39] Stankowski S 1984 Large ligand adsorption to membranes. III. Cooperativity and general ligand shapes *Biochim. Biophys. Acta* **777** 167–82
[40] Stankowski S 1983 Large ligand adsorption to membranes. II. Disc-like ligands and shape dependence at low saturation *Biochim. Biophys. Acta* **735** 352–60
[41] Trusova V 2012 Modulation of physiological and pathological activities of lysozyme by biological membranes *Cell Mol. Biol. Lett.* **17** 349–75